Measurement and comparison of dielectric properties of human pancreatic tumours, healthy tissues and porcine tissues ex vivo between 1Hz and 1MHz

Théo Le Berre, Julien Marchalot, Marie Frenea-Robin, Jérôme Cros, Frédéric Prat, Guilhem Rival

Bioelectrochemistry 161 (2025) 108821

Contents lists available at ScienceDirect

Bioelectrochemistry

journal homepage: www.journals.elsevier.com/bioelectrochemistry

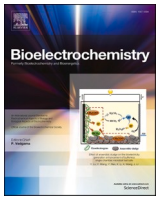

Measurement and comparison of dielectric properties of human pancreatic tumours, healthy tissues and porcine tissues *ex vivo* between 1Hz and 1MHz

Théo Le Berre [a,*], Julien Marchalot [a], Marie Frénéa-Robin [a], Jérôme Cros [b], Frédéric Prat [c,d], Guilhem Rival [e]

[a] Ecole Centrale de Lyon, INSA Lyon, Universite Claude Bernard Lyon 1, CNRS, Ampère, UMR5005, 69130 Ecully, France
[b] Dept of pathology, Beaujon hospital, Clichy, AP-HP, France
[c] Dept of endoscopy, Beaujon hospital, Clichy, AP-HP, France
[d] Université Paris-cité, France
[e] INSA Lyon, LGEF, UR682, 69621 Villeurbanne, France

ARTICLE INFO

Keywords:
Tissue dielectric properties
Ex vivo impedance measurement
Pancreatic tissue
Tumour-bearing tissues
Pancreatic cancer

ABSTRACT

The dielectric properties of pancreatic tissues from human healthy and tumour-bearing tissues have been extracted from impedance measurement on *ex vivo*, freshly excised samples. They are compared to pig pancreas samples, measured following the same protocol. The purpose is to add data to the scarce literature on the properties of the human pancreas and pancreatic tumours, for treatment planning, tissue identification and numerical simulations. The conductivity measured at 500 kHz for human healthy pancreas is 0.26 S/m, while the conductivity of tumour-bearing tissues is 0.44 S/m. Those values differ significantly from that listed in the IT IS database at 0.57 S/m, suggesting an update might be to consider. However, measures of relative permittivity are in accordance with the database with a value of approximately $2.3x10^3$. *Ex vivo* porcine model, while being less conductive than human pancreas with 0.16 S/m at the same frequency, is deemed a relevant model when studying pancreatic applications of electromagnetic fields-based treatments, such as radiofrequency ablation.

1. Introduction

The dielectric properties of human tissues are important to consider in the context of several biomedical applications, as they describe the way tissues behave in electromagnetic fields [1,2]. These applications cover treatments such as functional electrical stimulation, microwaves, radio frequency hyperthermia [3] or electroporation and other pulsed electric field-based treatments [4]. The analysis of these properties can also be used as a diagnostic tool: as they give a macroscopic image of cellular phenomena and structures, they can reflect a change in cellular properties or shapes, for example in the case of tumours [5–8]. These data are also used for the development of numerical models [9–12].

The properties of interest are the permittivity ε, describing the material's ability to oppose the application of the electric field and to store electrical energy, as well as the conductivity σ, associated in particular to the ability of a material to transport free charges and to the electrical loss through Joule heating. Biological samples are neither perfect conductors nor insulators, presenting both behaviours. Complex permittivity can thus be useful to represent conductivity and permittivity in a single complex quantity:

$$\underline{\varepsilon} = \varepsilon_0\varepsilon_r - j\frac{\sigma}{\omega} = \varepsilon^{'} - j\varepsilon^{''} \quad (1)$$

A complex conductivity can similarly be defined, linked to complex permittivity through:

$$\underline{\sigma} = j\omega\underline{\varepsilon} = \sigma^{'} + j\sigma^{''} \quad (2)$$

Biological tissues are heterogeneous materials, mainly composed of different types of cells tightly arranged within an extracellular medium. As such, in an electric field E, local polarization takes place at certain frequencies, inducing relaxations at the macroscopic level called dispersions, relative permittivity and conductivity of biological tissues are thus frequency-dependent. Dispersions are well described and explained in the literature [2,13]. The three major ones are named α, β and γ. The α dispersion observed in the low frequency region, below 10 kHz, results from the polarization of counter-ions near the charged surface of cell

* Corresponding author at: Ecole Centrale de Lyon, Laboratoire Ampère, Ecole Centrale de Lyon, 36 avenue Guy de Collongue, 69134 Ecully, France.
E-mail address: theo.le-berre@ec-lyon.fr (T. Le Berre).

https://doi.org/10.1016/j.bioelechem.2024.108821
Received 23 July 2024; Received in revised form 11 September 2024; Accepted 13 September 2024
Available online 17 September 2024

membranes. The β dispersion occurs at higher frequency, usually between 10 kHz to tens of MHz, due to Maxwell-Wagner interfacial polarisation effects related to the plasma membrane and its interaction with internal and external electrolytes. The γ dispersion mostly corresponds to the polarization of water molecules contained in the tissues, and typically appears above 10^9 Hz.

Numerous data on dielectric properties have been collected and reviewed over several decades from many organs and tissues, mainly by C. Gabriel and S. Gabriel and their team [14–17], and are freely available on regularly updated databases like IT'IS Foundation's. But in the case of pancreas only few data can be found, the IT'IS' data corresponding to thyroid gland for example [18]. Some measures do exist in small animal models (cats and dogs), but are difficult to extrapolate a priori to humans [19,20].

In this work, we present the data collected through impedance measurements on freshly excised human tumour-bearing pancreas after surgical procedures for locally advanced pancreatic cancer. Both healthy and tumour tissues were analysed, along with healthy samples from porcine pancreas, over a frequency range of 10 Hz to 1 MHz.

The aims of this study are to fill a gap in the literature dataset, to compare healthy and tumour tissues coming from the same patients and to assess the relevance of the porcine pancreas as a valid *ex vivo* replacement model for electromagnetic field-based therapies.

2. Material and methods

2.1. Ethical statement

All procedures involving identifiable human material were carried out in accordance with the Declaration of Helsinki. All patients whose resected material was used in this study were informed of the nature of the planned measures and gave their consent. For animal material, an administrative authorization was delivered by local authority (Prefecture du Rhône, DDPP-SPA 2023–321) to perform scientific experimentation on animal remains.

2.2. Sample acquisition

Human samples were provided by Beaujon hospital (AP-HP, Clichy, France) after non-objection for using medical waste was obtained from patients. Fresh tissue samples were collected within hours (usually less than 2 h) of surgery from patients undergoing partial resection of the pancreas, due to locally advanced cancer. Sample preparation was performed by a senior pathologist, who also identified the tissues as either healthy or tumour-bearing. The samples from seven patients in total were used in this study, the measurements took place in two sessions, on site. It is noteworthy that several patients had received chemotherapy and/or radiotherapy prior to surgery.

A third session of measurements was carried out on fresh samples of the pancreatic gland from five pigs intended for consumption, provided by the slaughterhouse Sopacel at Saint-Romain-de-Popey, France. Those measurements took place in Ampère laboratory, in Ecully. All pig pancreases were collected at the same time, in a bag provided by the slaughterhouse without particular medium. They were stored between 4 °C and 8 °C in a portable fridge for half an hour during transportation, and at the same temperature in the lab until measurement. Pancreases were taken out of the fridge and prepared into measurable samples at room temperature individually. For each animal, all measurements were performed within half an hour following the exposition to room temperature. The overall session took place in less than 4 h.

2.3. Measurements

Both human and porcine samples were first cut in approximately 2 mm thick slices, then shaped with a punch, when possible, for a reproducible surface, and with a scalpel otherwise. The final shape of the samples was highly dependent on the tissue stiffness and in most cases, the sample slice could not be approximated to a disc. In that case, the surface area was evaluated using a photograph of the sample placed on a paper grid, as shown on Fig. 1a. The image was analyzed with ImageJ software to estimate the surface area. The grid scale and manual contouring within the software enabled precise surface area measurement for each sample.

Samples were placed at room temperature on a sample holder (Solartron analytical, 12962a) between two parallel circular brass electrodes, pictured in Fig. 1b). The test bench being equipped with a caliper, the thickness of the samples was measured as the distance between the electrodes sandwiching them. The impedance measurement was performed using a PalmSens4, with a minimum frequency range of 10 Hz to 1 MHz. The input voltage was 0.25 V, and the minimum sampling time was set at 0.5 s (or 2 periods for a frequency below 4 Hz). The data collected were post-treated using Matlab® software.

It should be noted that all sample have different surface areas and thicknesses, which was taken into account when extracting the electrical properties from the impedance measurements.

2.4. – Preparation of reference samples

Agarose discs (2 %) were prepared from a saline solution (KCl, Conductivity standard 1413 $\mu S/cm$, from Mettler-Toledo) as test samples. These samples were measured using the same approach described in section 2.3 to assess their conductivity across the spectrum. The experiment was conducted on five different agarose discs.

2.5. – Statistics

Normal distribution of each series was checked using a Shapiro-Wilk test with a significance level of 5 %, adapted to dataset with a low number of points. It was therefore verified that each group of measurement follows a normal distribution, with a group defined as all spectra measured for one animal or patient, considering healthy and tumour-bearing tissues separately. It is to be noted that the three datasets "all pig sample", "all human healthy samples" and "all human tumour-bearing samples" are not expected to follow a normal distribution, as they are the concatenation of normal distributions with different means. In our case, among those three, only the "all human tumour-bearing samples" dataset was found to have normally distributed data according to the Shapiro-Wilk test.

Thus, when comparing the means of two datasets, the p-values calculated corresponds to a Wilcoxon rank sum test, adapted to non-normal distribution with a low number of points. The null hypothesis states that the two series come from continuous distributions with equal means, tested at 5 % significance level. Thus, if $p < 0.05$ the null hypothesis is rejected and it can be concluded with 95 % confidence that the means are significantly different. For comparing variances, the p-value were calculated using the Levene test, where the null hypothesis assumes that the two distribution have equal variance. If $p < 0.05$ this hypothesis is rejected indicating with 95 % confidence that the variances are significantly different. The Wilcoxon rank sum test and Levene test were performed using Matlab software.

When comparing more than two series, the p-value was calculated using an ANOVA test, under the hypothesis that all series come from normal distribution with equal means, tested at 5 % significance level. If $p < 0.05$ this hypothesis is rejected with 95 % confidence, indicating that at least one of the series has a mean significantly different from the others. The ANOVA test was applied only to datasets that were confirmed to follow a normal distribution and was performed with Excel software.

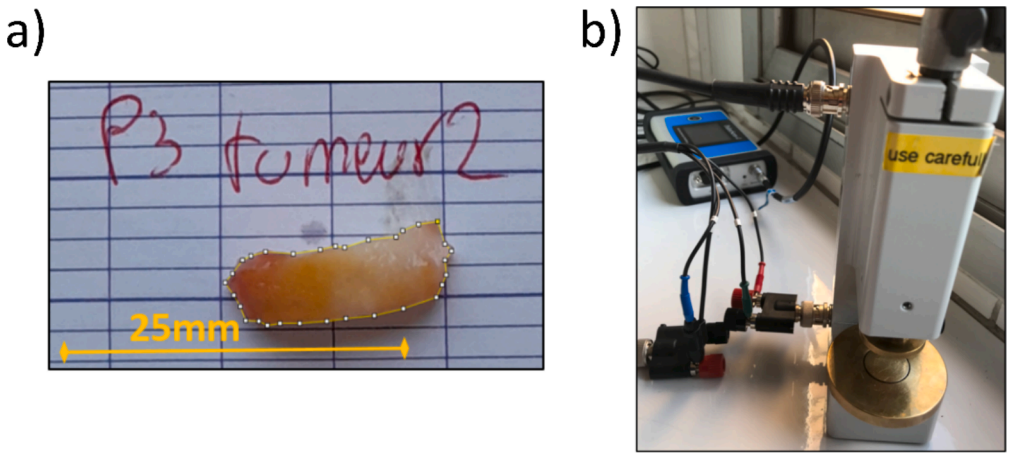

Fig. 1. A) picture of the second tumorous sample of patient 3, on gridded paper to measure the surface of the sample b) picture of the experimental setup, with the sample holder (solartron analytical, 12962a) and the impedance analyser (palmsens4).

3. Theory/Calculation

3.1. – Data extraction

Electrical impedance is the ratio between the alternative voltage applied on the sample and the out-of-phase alternative current resulting from this application. The applied voltage can be expressed as:

$$V(t) = V_0\cos(\omega t) \tag{3}$$

Where V_0 is the amplitude of the signal, and ω is the angular frequency $\omega = 2\pi f$. In a linear system, the response signal, I(t), is shifted in phase and can be expressed as:

$$I(t) = I_0\cos(\omega t - \Phi) \tag{4}$$

To define the impedance of the dipole, we introduce the two phasors:

$$\underline{V} = V_0 e^{j\omega t} \tag{5}$$

$$\underline{I} = I_0 e^{-j\Phi} e^{j\omega t} = I_0 e^{j(\omega t-\Phi)} \tag{6}$$

V(t) and I(t) are then the real parts of $\underline{V}$ and $\underline{I}$, respectively.

For a linear component, impedance can be defined as the ratio of the phasor for the voltage across the component and the current through the component:

$$\underline{Z}(\omega) = \frac{\underline{V}(\omega)}{\underline{I}(\omega)} = \frac{V_0}{I_0}e^{j\Phi} = Z'(\omega) - jZ''(\omega) \tag{7}$$

The impedance magnitude can therefore be expressed (in ohms) as:

$$\left|\underline{Z}\right| = \frac{V_0}{I_0} \tag{8}$$

And its phase is given by:

$$\arg\left(\underline{Z}\right) = arctan(-Z''/Z') \tag{9}$$

Complex permittivity or complex conductivity can be linked to impedance in the simple case of two parallel face-to-face electrodes, through the equation:

$$\underline{Z}(\omega) = \frac{d}{j\omega\underline{\varepsilon}S} = \frac{d}{\underline{\sigma}S} \tag{10}$$

Where S is the surface area of the sample and d its thickness.

We can therefore write the equations linking the measured impedance to the sample dielectric properties:

$$\begin{cases} \sigma' = \sigma = \dfrac{d}{S}\dfrac{Z'}{|Z|^2} \\ \sigma'' = \omega\varepsilon_0\varepsilon_r = \dfrac{d}{S}\dfrac{Z''}{|Z|^2} \\ \varepsilon' = \varepsilon_0\varepsilon_r = \dfrac{d}{S\omega}\dfrac{Z''}{|Z|^2} \\ \varepsilon'' = \dfrac{\sigma}{\omega} = \dfrac{d}{S\omega}\dfrac{Z'}{|Z|^2} \end{cases} \tag{11}$$

4. – Results

4.1. Measurement device validation

The real part of the impedance obtained for one of the samples is presented in Fig. 2.

At the room temperature (27 °C), the expected conductivity of the solution was 0.146 S/m. At the two frequencies of interest in this study, 10 kHz and 500 kHz, the evaluated conductivity were respectively 0.12 ± 0.01 S/m and 0.15 ± 0.02 S/m. The relative errors in mean values were 17 % at 10 kHz and 4 % at 500 kHz. Therefore, the measurement system is considered acceptable in terms of precision, at the studied frequencies.

The greater relative error at 10 kHz can be explained by the effect of

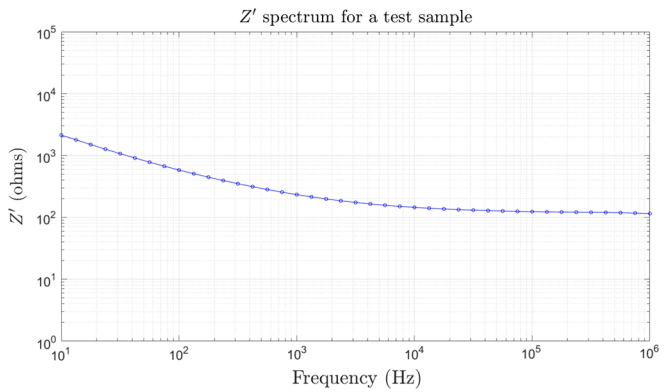

Fig. 2. Spectrum of Z' measured for one of the agarose test samples.

the double layer, which is still slightly present, as can be seen on Fig. 2.

4.2. General overview

All raw data are provided as supplementary material. They are presented in the form of a table per sample containing frequency, norm of the impedance, phase of the impedance, real part and imaginary part of the impedance. All sample areas and thicknesses are listed in a separate table. An example of the collected data is presented in Fig. 3, for patient 1 (healthy and malignant tissues) and pig 1, as the measured norm and phase of the impedance.

Overall, samples from five pigs and seven human patients, either malignant or healthy pancreatic tissue, were used in this study for a total of 28 pigs' samples, 18 humans' samples of healthy pancreas, and 15 samples of pancreatic ductal adenocarcinoma (PDAC). Table 1presents an overview of the samples measured, the "patient information" column is an indication in particular of patient treatment, if they had received chemotherapy and/or radiotherapy before surgery, or not.

4.3. Extracted electrical properties

The properties were extracted from the impedance measurements using the methodology described in section 3. Fig. 4 presents the real and imaginary parts of conductivity and permittivity as defined in equation (11) for human, healthy and malignant tissues. As in Fig. 3, only the data for patient 1 is plotted for readability purpose.

Fig. 5 presents the real and imaginary parts of conductivity and permittivity as defined in equation (11) for pigs. As in Fig. 3, only the data for pig 1 is plotted for readability purpose.

4.4. Properties at specific frequencies

For the sake of clarity, two frequencies of interest have been selected to be highlighted. Fig. 6 thus presents the comparison in properties at 10 kHz of the groups "Porcine pancreas", "Healthy human pancreas" and "Tumorous human pancreas", along with a comparison of each animal within the "Porcine pancreas" group. The choice of this frequency is justified in the discussion section.

Fig. 7 presents the same comparison at 500 kHz, which is the usual frequency of interest for radio-frequency ablation procedures [10].

Mean values and standard deviations for conductivity and relative permittivity are summarised in Table 2, at 10 kHz and 500 kHz.

5. Discussion

5.1. General observations

Tumour tissues were found to be significantly different from those identified as healthy in the patients' pancreas, which was expected as the conductivity is known to be higher in tumour tissues. Their behaviour is overall a little less resistive, as we can see in Fig. 3 that the phase is regularly higher across the spectrum for patient 1, and in Fig. 4 that the value of the relative permittivity increases. This tendency was also visible in the other samples form patients, and is consistent with the literature for other tissues [6].

5.2. Electrode polarization

It is to be noted that the two-electrode configuration used for these measurements, if the simplest, is not the most accurate to directly evaluate the properties of samples at low frequency. Indeed, the phenomenon of electrode polarization as to be taken into account. At the electrode–electrolyte interface, no electron exchange can take place, as electrons cannot pass into the solution. Consequently, any excess charge in the electrode tends to be compensated by ions in the electrolyte. This creates what is known as the electrical double layer, which can be modelled as a first step by a capacitor (known as the Helmoltz model), and be refined to a constant phase element (CPE) to take into account its imperfect capacitive nature [21]. Other more complex model do exist, taking into account in particular the distribution of ions across the layer.

This double-layer impedance is dominant at low frequencies, and may distort the intended measurement. The measured impedance can be written as:

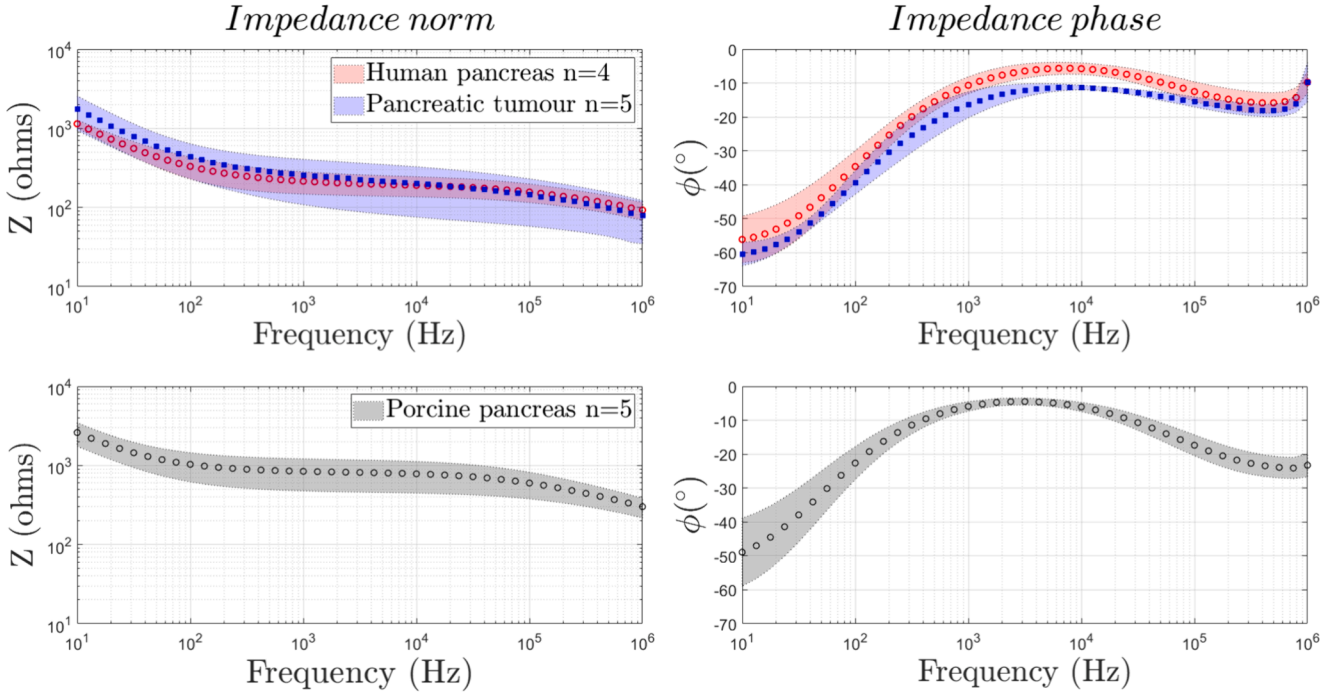

Fig. 3. Impedance spectrum, in norm and phase, of patient 1 samples, healthy and tumorous (above, respectively red circles and blue squares) and of pig 1 (below). The markers indicates the mean value, and the coloured area the mean value plus and minus the standard deviation.

Table 1
Overview of the samples studied. In the present series, all human patients had received both chemo ad radiotherapy.

Source	ID	Type	Number of sample	Patient information
Pig samples	Pig 1	Healthy	6	/
	Pig 2	Healthy	6	/
	Pig 3	Healthy	6	/
	Pig 4	Healthy	5	/
	Pig 5	Healthy	12	/
Human samples	Patient 1	Tumour	5	No information
		Healthy	4	
	Patient 2	Tumour	3	77-year-old man; mixed IPMN (intrapapillary pancreatic mucinous neoplasm) of predominantly gastric phenotype in low-grade dysplasia with high-grade microfocus, extending 3 cm in length. No pre- or post-operative treatment.
		Healthy	3	
	Patient 3	Tumour	2	65-year-old man; first operated in 2019 for an adenocarcinoma developed on IPMN (intrapapillary pancreatic mucinous neoplasm) with left splenopancreatectomy followed by 6 months of adjuvant chemotherapy with FOLFIRINOX. Recurrence in 2023, undergoing iterative pancreatic resection by enlarged pancreatectomy. No radiotherapy or chemotherapy before the 2nd surgery.
		Healthy	2	
	Patient 4	Tumour	3	60-year-old man; grade 1 sporadic non-functioning neuroendocrine tumor (NET), treated by distal (left) pancreatectomy without splenectomy. No pre- or post-operative treatment.
		Healthy	3	
	Patient 5	Tumour	1	74-year-old man. Well-differentiated ductal adenocarcinoma extending over 18 mm. Treatment with preoperative chemotherapy.
		Healthy	1	
	Patient 6	Tumour	3	27-year-old man; Very marked inflammatory processes in the periampullary region, with numerous lymph nodes with necrotic granulomatous lesions and fibrous changes.
	Patient 7	Tumour	2	76-year-old man; poorly differentiated ductal adenocarcinoma (25 mm). Treatment with preoperative chemotherapy.
		Healthy	2	

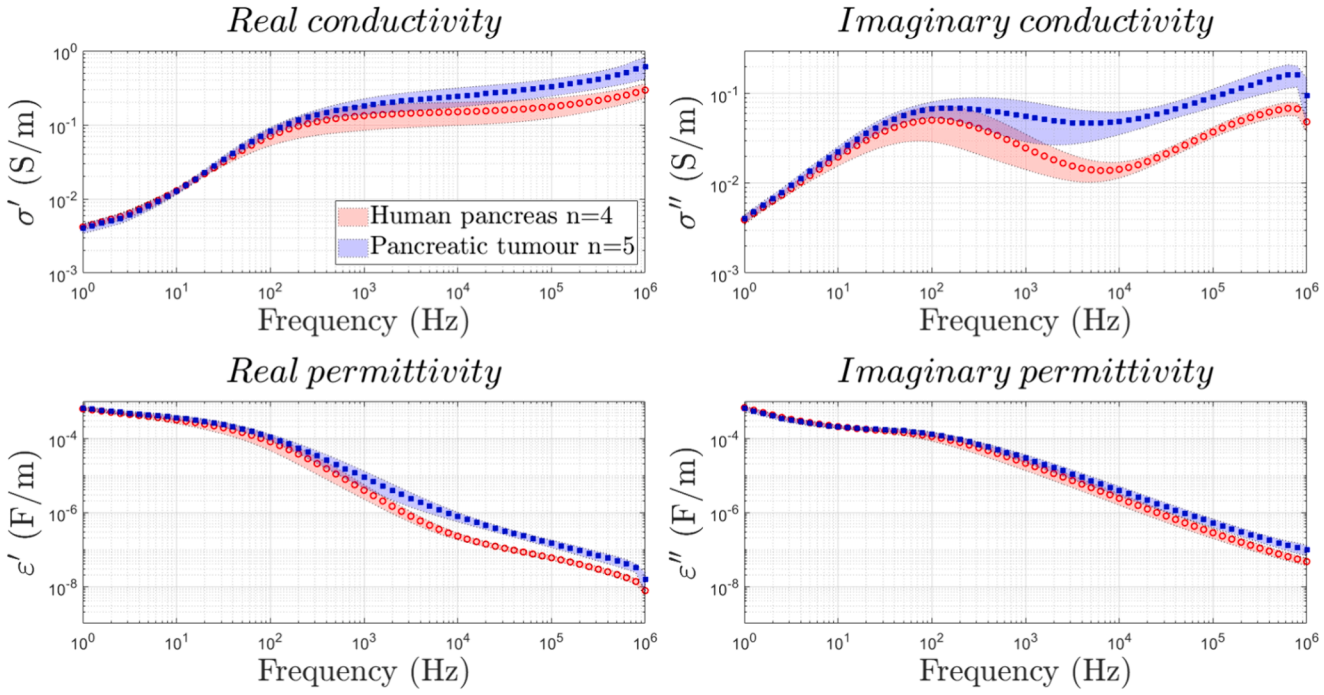

Fig. 4. Complex conductivity and permittivity spectra of patient 1 samples, healthy (red circles) and tumorous (blue squares). The markers indicate the mean value, and the coloured area the mean value plus/minus the standard deviation.

$$\underline{Z}_{measured} = \underline{Z}_{interface} + \underline{Z}_{sample} \quad (12)$$

Experimentally, it is considered that for *in vivo* measurements with two electrodes the data collected are reliable above 1 kHz [2]. As we can see in Fig. 3, while the impact of the double layer seems negligible at this frequency on pig samples, this is not completely the case for the different human samples. In order to keep a safety margin in the comparison of properties, the lower frequency of interest was fixed at 10 kHz.

5.3. Intra –pancreas inhomogeneity, and inter-individual variations

We can see on the pig samples, supposedly the most regular dataset, as the animals were all similarly raised for human consumption and healthy, that a significant difference in properties can be noted between each animals, and between samples from the same animal.

As all the samples were collected fresh on the same day, and stored in parallel in the same conditions, it was expected that the measured properties would not be highly different from one animal to another. However it appears that both at 10 kHz and 500 kHz, the differences are significant for conductivity ($p = 10^{-5} < 0.05$ at 10 kHz according to ANOVA test and $p = 10^{-5} < 0.05$ at 500 kHz) as well as for relative permittivity ($p = 2 \times 10^{-4} < 0.05$ at 10 kHz according to ANOVA test and $p = 9 \times 10^{-4} < 0.05$ at 500 kHz). The mean values vary from 0.21 S/m to 0.50 S/m approximately for the conductivity, and from 9.3×10^{3} to 1.63

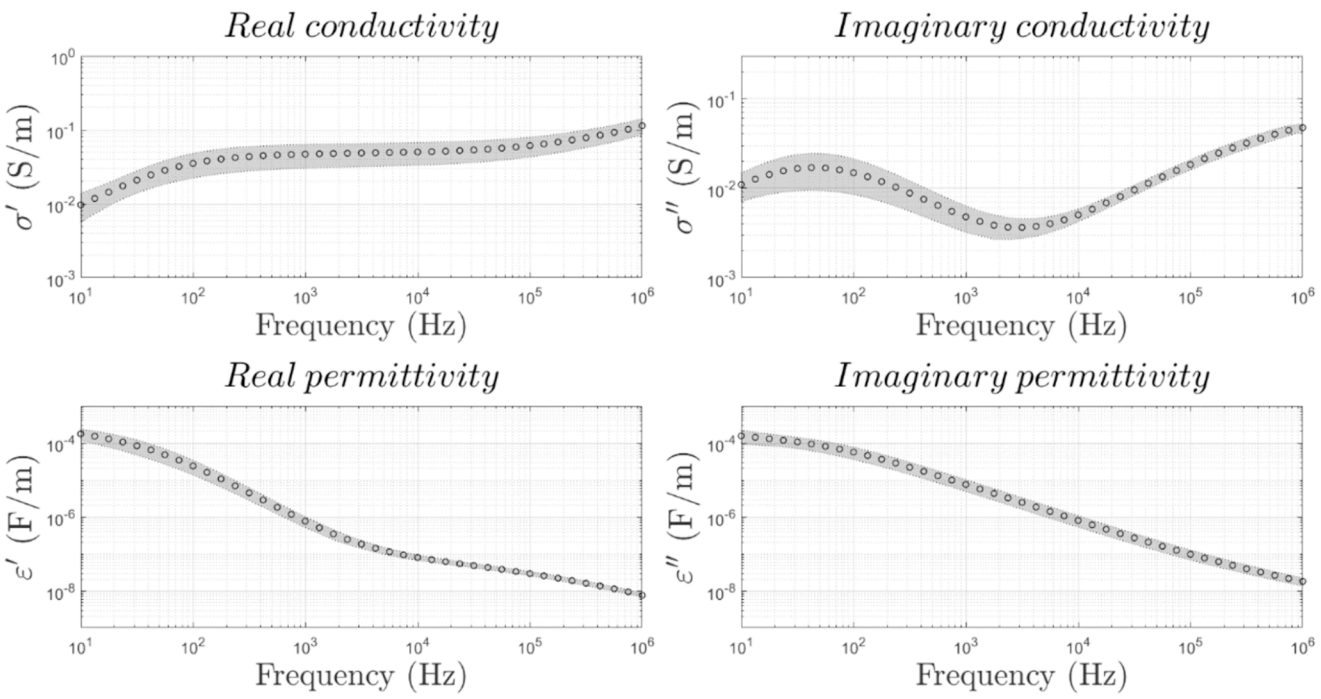

Fig. 5. Complex conductivity and permittivity spectra for pig 1 samples (n = 5). The markers indicate the mean value, and the coloured area the mean value plus/minus the standard deviation.

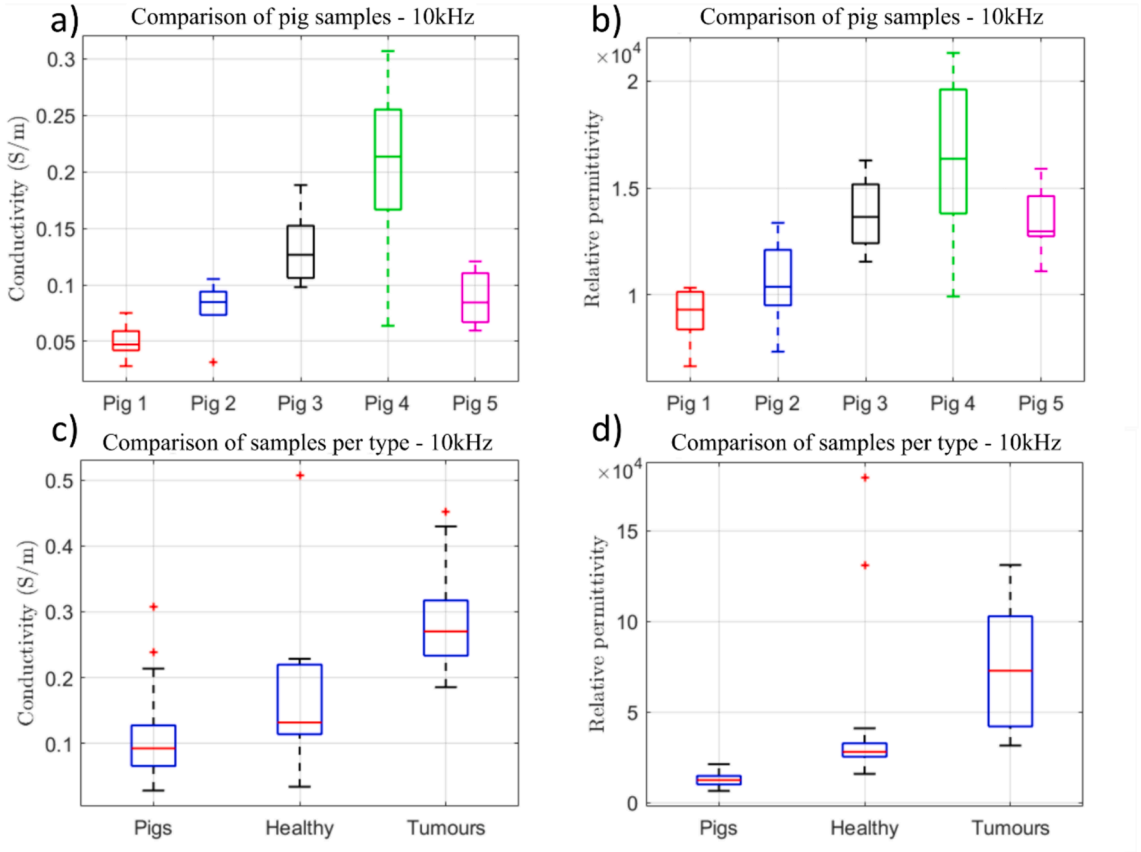

Fig. 6. Boxplot of properties of samples at 10 kHz. a) Comparison of extracted conductivities for pig samples. b) Comparison of extracted relative permittivities for pig samples. c) Comparison of extracted conductivities for all samples per type. d) Comparison of extracted relative permittivities for all samples per type.

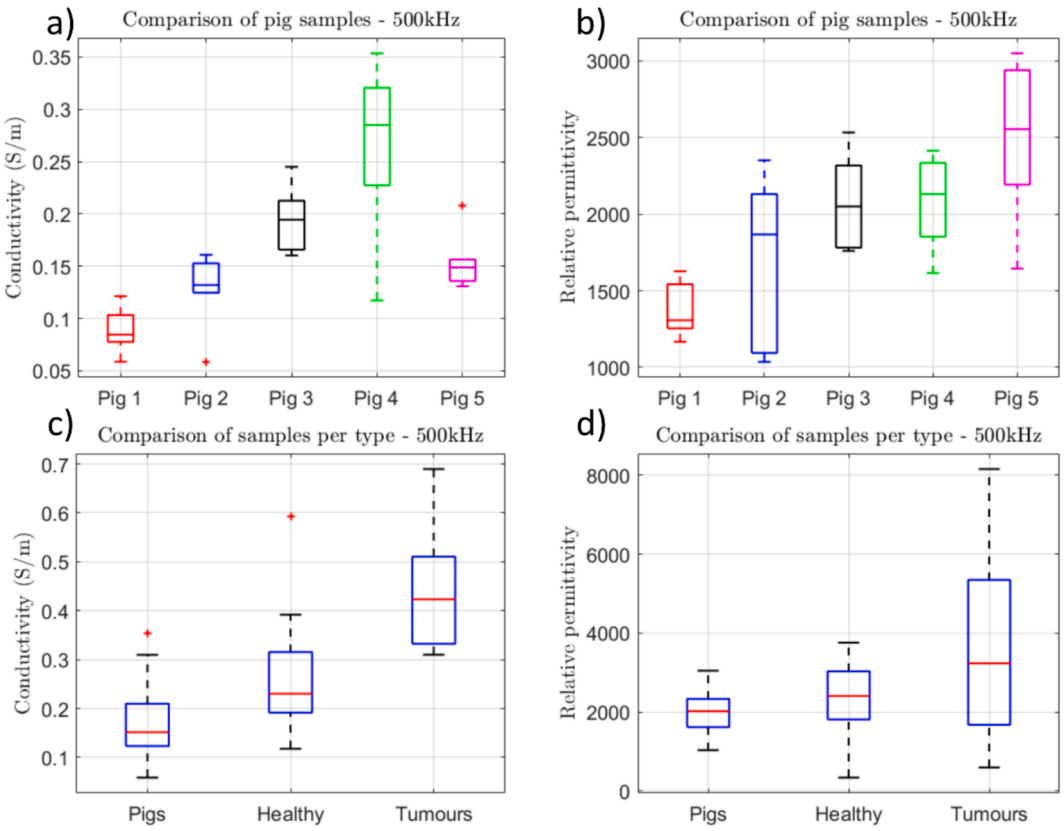

Fig. 7. Boxplot of properties of samples at 500 kHz. a) Comparison of extracted conductivities for pig samples. b) Comparison of extracted relative permittivities for pig samples. c) Comparison of extracted conductivities for all samples per type. d) Comparison of extracted relative permittivities for all samples per type.

Table 2
Summary of mean values measured for each type of tissue at 10 kHz and 500 kHz, with standard deviation.

10 kHz	Conductivity (S/m)	Relative permittivity
Porcine pancreas	0.11 ± 0.06	(1,27 ± 0,31) x 104
Human pancreas	0.16 ± 0.10	(4,15 ± 4,26) x 10^4
Tumorous tissues	0.29 ± 0.08	(7,46 ± 3,37) x 10^4
500 kHz	Conductivity (S/m)	Relative permittivity
Porcine pancreas	0,16 ± 0,07	(2,05 ± 0,57) x 10^3
Human pancreas	0,26 ± 0,11	(2,33 ± 0,98) x 10^3
Tumorous tissues	0,44 ± 0,11	(3,56 ± 2,12) x 10^3

x10^4 for relative permittivity.

The variation within the same animal can also be important, as observed for pig 4 at 10 kHz, where the ratio between the most and least conductive samples is nearly 3. Considering relative permittivity, this ratio equals approximately 2 on the same animal, whose intra-pancreatic properties were the most variable by far at this frequency. This inhomogeneity of tissue properties can be partially attributed to fat distribution within this organ [2,19].

For humans, there is a lack of data per patient to measure it, but the electrical properties of healthy pancreatic tissues are also expected to be heterogeneous in the organ, and to vary significantly among patients with different ages and lifestyle [2].

5.4. Comparison of human healthy and tumorous tissues

For a clearer comparison between healthy pancreas and tumour-bearing tissues, Fig. 8 presents the quartiles of the populations' properties between 10 kHz and 1 MHz. The mean values are presented in Table 2 for 10 kHz and 500 kHz, along with the standard deviations.

The comparison between human sample types shows that tumour tissues as a mean value are approximately two-fold more conductive than healthy ones, with 0.16 S/m for healthy pancreas and 0.29 S/m for tumours at 10 kHz. The ratio is slightly lower at 500 kHz, with 0.26 S/m for healthy pancreas and 0.44 S/m for tumours. The difference is conductivity between the two populations is significant in the frequency range from 10 kHz to 1 MHz, as seen in Fig. 8.

In terms of relative permittivity, at 10 kHz, the mean value for tumorous tissues of 7.46 x10^4 is significantly higher than the mean value for healthy tissues of 4.15 x10^4. The difference is nevertheless not significant at 500 kHz, with a variation from 2.33 x10^3 for healthy tissues to 3.56 x10^3 for tumorous tissues. As we can see in Fig. 8, the difference in terms of relative permittivity between the two populations becomes non-significant at 30 kHz, and remains so up to 1 MHz.

Differences in properties at macroscopic level between healthy and tumour tissues were expected from the changes in properties at the cellular level, in size, membrane area and capacitance [8,22].

As presented tumours have different types, and tumorous tissues are notoriously more chaotic in structure, the variability of tumours properties was expected to be higher than that of healthy tissues. This seems to be true for relative permittivity, but false for conductivity, as the two distributions present a comparable variance along the spectrum.

Overall, the properties measured for the human pancreas are comparable in order of magnitude to other organ such as kidney, bladder or liver, as reported in the literature [14].

It is interesting to note that the values measured for conductivity are different from the values usually presented in the IT'IS database, and the IFAC-CNR database. As no measurements for pancreas have been published for human, they both use thyroid gland tissues as a reference tissue for the pancreas, supposedly because of similarity of the tissues. At 500 kHz, the conductivity is 0.566 S/m according to the databases. The mean conductivity presented in this work for human pancreas at the same frequency is less than half that value, with 0.256 S/m, which is

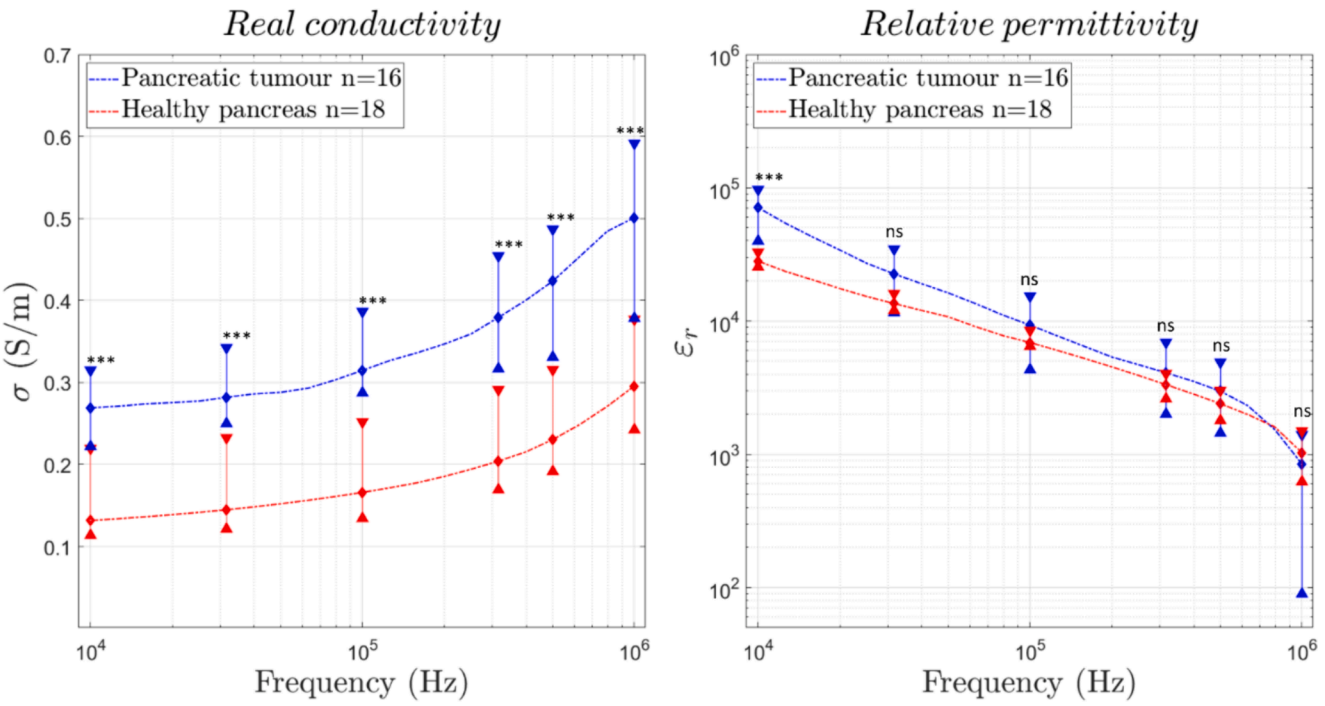

Fig. 8. Plot of the extracted conductivity and relative permittivity of the healthy humans pancreases and tumour-bearing tissues, presented in quartiles. The triangle shaped markers representing the first quartile at a given frequency, the diamond shaped markers representing the median, and the reverse triangle shaped markers representing the third quartile. *** $p < 0.001$ and 'ns' for non-significant ($p > 0.05$) according to the Wilcoxon rank sum test.

surprisingly close to the values that can be found in old papers on cat tissues [19], with approximately 0.286 S/m (read as 350 Ω.cm at 500 kHz) and on dog tissues [20], with 0.268 S/m at 254 kHz. However the differences in conditions of conservation of the tissues and methodology forces to be careful with this comparison, as measurements on cats were performed *in vivo* under anaesthesia, and measurements on dogs were performed *ex vivo* in the 12 h following death, with no details on the conditions of conservation.

This substantial difference with the databases suggests that the pancreatic conductivity value usually used might need to be updated. On the other hand, the relative permittivity evaluated in this work of 2.33×10^3 at 500 kHz seems in agreement with the value 2.14×10^3 listed in the databases at the same frequency.

5.5. Comparison of human and porcine healthy tissues

At 10 kHz, the porcine tissues are slightly but significantly ($p = 4 \times 10^{-3} < 0.05$) less conductive than human healthy pancreatic samples, with a mean value of 0.11 S/m for pigs, and 0.16 S/m for human. The difference increases at 500 kHz, with a value of 0.16 S/m for pigs, and 0.26 S/m for humans, and stays significant ($p = 5 \times 10^{-4} < 0.05$).

For relative permittivity, the value is also significantly lower for porcine tissues at 10 kHz with a value of 1.27×10^4 compared to a value of 4.15×10^4 for human samples ($p = 10^{-8} < 0.05$). However the values are close at 500 kHz, with 2.05×10^3 for porcine pancreas and 2.33×10^3 for humans. There is no significant difference ($p = 0.08 > 0.05$) at this frequency between the two series of measurement.

It is interesting to see that variances in conductivity of the groups "Healthy pancreas" and "Porcine pancreas" cannot be considered to be significantly different according to Levene's test ($p = 0.14 > 0.05$ at 10 kHz and $p = 0.09 > 0.05$ at 500 kHz). We can thus consider that in term of conductivity, the repartition of properties expected for a human population is comparable to that represented by this porcine population.

On the other hand, there is a significant difference in variances between those two groups when considering relative permittivity ($p = 2 \times 10^{-4} < 0.05$ at 10 kHz and $p = 0.02 < 0.05$ at 500 kHz), the variance for human samples being slightly greater.

6. Limitations

A number of limitations must be taken into consideration when interpreting the findings of this study. First of all, one limitation relates to the nature of the samples, which are fresh *ex vivo* samples at room temperature. These data are less reliable than *in vivo* measurements. Moreover, most human tissues studied here were exposed to chemotherapy and/or radiotherapy beforehand, with different modalities. As a consequence, the values extracted for conductivity and relative permittivity cannot be used for healthy tissues as well as for untreated PDAC without caution. However, given the lack of literature on this organ, these measurements can be considered a good first assessment of pancreatic tissue properties. It is also to be noted that the properties measured are those of the tissues prior to any electromagnetic-based treatment, and the modifications that might be caused by any therapy in the tissues are not measured here.

Another point is the method used. As mentioned previously, the two-electrode method is not ideal for data collection, and even if the electrode polarization can be analytically removed [23], a four-electrode configuration should be considered for further measurements.

Lastly, the impedance analyser used limited frequency range, and if adapted to radio-frequency ablation applications (at around 500 kHz) the data collected are not high-frequency enough for some other applications, such as microwave ablation (at 915 MHz or 2.45 GHz), or some numerical models dedicated to dosimetry. For those applications, one could only consider these data a low frequency basis for comparisons of pancreatic tissues with other tissues previously described in the literature.

7. Conclusion and perspectives

This work adds new data to the literature on the electric properties of pancreatic tissues. The procedure implying several samples per patient and animal presented in this study allows to observe the significant

disparity in properties between and within each individual. In terms of mean values, a tumour-bearing tissue was found to be approximately two-fold more conductive than a healthy pancreatic tissue, with a 2.6 times higher relative permittivity. The values of conductivity measured in this work are significantly different than those listed in reference databases, suggesting that the reference values might need to be updated. The relative permittivity measured is however in accordance with the databases.

It is interesting to note that the inter-individual variation was comparable between human and porcine pancreas, making the latter a relevant and much more accessible model when planning or studying the effects of a treatment, as well as for monitoring electromagnetic-based therapies targeting the pancreas. The differences in conductivity should nevertheless be taken into account as porcine pancreases exhibited properties that differed from the human samples they were compared to, although they were of comparable magnitude.

In the future, it would be interesting to complete those data with post-treatment measurements, especially in the cases of radiofrequency ablation and electroporation. One of the main challenge with RF-ablation modelling being the changes in properties with the temperature (up to 100 °C) [10], and for electroporation the physiological changes caused by the procedure [24], depending on the electric field applied. In both cases, a comparison of properties in a given tissue pre and post treatment could bring interesting insights in the comprehension of the physiological phenomena and their numerical modelling.

CRediT authorship contribution statement

Théo Le Berre: Writing – original draft, Validation, Formal analysis, Data curation, Conceptualization. **Julien Marchalot:** Writing – review & editing, Supervision, Funding acquisition. **Marie Frénéa-Robin:** Writing – review & editing, Supervision, Funding acquisition. **Jérôme Cros:** Writing – review & editing, Resources, Investigation. **Frédéric Prat:** Writing – review & editing, Project administration, Funding acquisition. **Guilhem Rival:** Writing – review & editing, Supervision, Investigation.

Declaration of competing interest

The authors declare that they have no known competing financial interests or personal relationships that could have appeared to influence the work reported in this paper.

Data availability

All raw data are in the .mat file provided as supplementary material at the “attached files” step.

Acknowledgment

Funding: This work was carried out as part of the Impulse project supported by the Institut Carnot Ingenierie@Lyon. The authors gratefully acknowledge financial support from ITMO Cancer of Aviesan within the framework of the 2021-2030 Cancer Control Strategy, on funds administrated by Inserm, France. This project has also received financial support from the CNRS through the MITI interdisciplinary programs through its exploratory research program.

The authors would also like to thank Alain Sauvanet, MD, PhD and Safi Dokmak, MD, PhD from the department of HPB surgery of Beaujon hospital, for assistance with sample collection, and Jérôme Cros, MD, PhD from the department of pathology of Beaujon hospital, for processing of the samples and identification.

We sincerely thank the reviewers for their relevant comments.

Appendix A. Supplementary data

Supplementary data to this article can be found online at https://doi.org/10.1016/j.bioelechem.2024.108821.

References

[1] R. Pethig, Dielectric Properties of Biological Materials: Biophysical and Medical Applications, IEEE Trans. Elect. Insul. EI-19 (1984) 453–474. https://doi.org/10.1109/TEI.1984.298769.
[2] D. Miklavčič, N. Pavšelj, F.X. Hart, Electric Properties of Tissues, in: Wiley Encyclopedia of Biomedical Engineering, John Wiley & Sons, Ltd, 2006. https://doi.org/10.1002/9780471740360.ebs0403.
[3] V. Granata, R. Grassi, R. Fusco, A. Belli, R. Palaia, G. Carrafiello, V. Miele, R. Grassi, A. Petrillo, F. Izzo, Local ablation of pancreatic tumors: State of the art and future perspectives, WJG 27 (2021) 3413–3428, https://doi.org/10.3748/wjg.v27.i23.3413.
[4] B. Geboers, H.J. Scheffer, P.M. Graybill, A.H. Ruarus, S. Nieuwenhuizen, R.S. Puijk, P.M. van den Tol, R.V. Davalos, B. Rubinsky, T.D. de Gruijl, D. Miklavčič, M. R. Meijerink, High-Voltage Electrical Pulses in Oncology: Irreversible Electroporation, Electrochemotherapy, Gene Electrotransfer, Electrofusion, and Electroimmunotherapy, Radiology 295 (2020) 254–272, https://doi.org/10.1148/radiol.2020192190.
[5] B. Blad, P. Wendel, M. Jonsson, K. Lindstrom, An electrical impedance index to distinguish between normal and cancerous tissues, Journal of Medical Engineering & Technology 23 (1999) 57–62, https://doi.org/10.1080/030919099294294.
[6] S. Laufer, A. Ivorra, V.E. Reuter, B. Rubinsky, S.B. Solomon, Electrical impedance characterization of normal and cancerous human hepatic tissue, Physiol. Meas. 31 (2010) 995, https://doi.org/10.1088/0967-3334/31/7/009.
[7] D. Haemmerich, S.T. Staelin, J.Z. Tsai, S. Tungjitkusolmun, D.M. Mahvi, J. G. Webster, *In vivo* electrical conductivity of hepatic tumours, Physiol. Meas. 24 (2003) 251–260, https://doi.org/10.1088/0967-3334/24/2/302.
[8] P. Gascoyne, S. Shim, Isolation of Circulating Tumor Cells by Dielectrophoresis, Cancers 6 (2014) 545–579, https://doi.org/10.3390/cancers6010545.
[9] T. Nagaoka, T. Togashi, K. Saito, M. Takahashi, K. Ito, T. Ueda, H. Osada, H. Ito, S. Watanabe, An anatomically realistic voxel model of the pregnant woman and numerical dosimetry for a whole-body exposure to RF electromagnetic fields, in: 2006 International Conference of the IEEE Engineering in Medicine and Biology Society, IEEE, New York, NY, 2006: pp. 5463–5467. https://doi.org/10.1109/IEMBS.2006.260807.
[10] E.J. Berjano, Theoretical modeling for radiofrequencyablation: state-of-the-art and challenges for the future, BioMed Eng OnLine 5 (2006) 24, https://doi.org/10.1186/1475-925X-5-24.
[11] O. Gallinato, B.D. De Senneville, O. Seror, C. Poignard, Numerical workflow of irreversible electroporation for deep-seated tumor, Phys. Med. Biol. 64 (2019) 055016, https://doi.org/10.1088/1361-6560/ab00c4.
[12] D. Voyer, A. Silve, L.M. Mir, R. Scorretti, C. Poignard, Dynamical modeling of tissue electroporation, Bioelectrochemistry 119 (2018) 98–110, https://doi.org/10.1016/j.bioelechem.2017.08.007.
[13] J.P. Reilly, Applied Bioelectricity, Springer, New York, New York, NY (1998), https://doi.org/10.1007/978-1-4612-1664-3.
[14] C. Gabriel, S. Gabriel, E. Corthout, The dielectric properties of biological tissues: I. Literature survey, (n.d.) 20.
[15] S. Gabriel, R.W. Lau, C. Gabriel, The dielectric properties of biological tissues: II. Measurements in the frequency range 10 Hz to 20 GHz, Phys. Med. Biol. 41 (1996) 2251–2269. https://doi.org/10.1088/0031-9155/41/11/002.
[16] S. Gabriel, R.W. Lau, C. Gabriel, The dielectric properties of biological tissues: III. Parametric models for the dielectric spectrum of tissues, Phys. Med. Biol. 41 (1996) 2271–2293. https://doi.org/10.1088/0031-9155/41/11/003.
[17] C. Gabriel, A. Peyman, Dielectric Properties of Biological Tissues; Variation With Age, in: Conn’s Handbook of Models for Human Aging, Elsevier, 2018: pp. 939–952. https://doi.org/10.1016/B978-0-12-811353-0.00069-5.
[18] C. Baumgartner, P.A. Hasgall, F. Di Gennaro, E. Neufeld, B. Lloyd, M.C. Gosselin, N. Kuster, Tissue Properties Database V4 (2024) 2, https://doi.org/10.13099/VIP21000-04-2.
[19] D.G. Clark, J.R. Greenwell, A.A. Harper, A.M. Sankey, T. Scratcherd, The electrical properties of resting and secreting pancreas, The Journal of Physiology 189 (1967) 247–260, https://doi.org/10.1113/jphysiol.1967.sp008166.
[20] R D Stoy, K R Foster, H P Schwan, Dielectric properties of mammalian tissues from 0.1 to 100 MHz; a summary of recent data, Pmb 27 (1982) 501–513. https://doi.org/10.1088/0031-9155/27/4/002.
[21] E.T. McAdams, A. Lackermeier, J.A. McLaughlin, D. Macken, J. Jossinet, The linear and non-linear electrical properties of the electrode-electrolyte interface, Biosensors and Bioelectronics 10 (1995) 67–74, https://doi.org/10.1016/0956-5663(95)96795-Z.

[22] M. Al Ahmad, Z. Al Natour, F. Mustafa, T.A. Rizvi, Electrical Characterization of Normal and Cancer Cells, IEEE Access 6 (2018) 25979–25986. https://doi.org/10.1109/ACCESS.2018.2830883.
[23] M. Samet, A. Kallel, A. Kallel-Elloumi, E. Drockenmuller, A. Serghei, Exchange Process in the Dielectric Loss of Molecular and Macromolecular Ionic Conductors in the Interfacial Layers Formed by Electrode Polarization Effects, J. Phys. Chem. B 123 (2019) 8532–8542, https://doi.org/10.1021/acs.jpcb.9b05837.
[24] T. García-Sánchez, D. Voyer, C. Poignard, L.M. Mir, Physiological changes may dominate the electrical properties of liver during reversible electroporation: Measurements and modelling, Bioelectrochemistry 136 (2020) 107627, https://doi.org/10.1016/j.bioelechem.2020.107627.